Separation and Purification Technology 386 (2026) 136571

Contents lists available at ScienceDirect

Separation and Purification Technology

journal homepage: www.elsevier.com/locate/seppur

Integrated experimental, process simulation, and techno-economic assessment of biogas upgrading via pressure/vacuum swing adsorption

Mohsen Karimi [a,b,*], Rafael M. Siqueira [a,b,c], Mohammad Shirzad [a,b], Alexandre F.P. Ferreira [a,b], Alírio E. Rodrigues [a,b], José A.C. Silva [d,e]

[a] Laboratory of Separation and Reaction Engineering (LSRE), Associate Laboratory LSRE/LCM, Faculty of Engineering, University of Porto, Rua Dr. Roberto Frias, 4200-465 Porto, Portugal
[b] ALiCE - Associate Laboratory in Chemical Engineering, Faculty of Engineering, University of Porto, Rua Dr. Roberto Frias, 4200-465 Porto, Portugal
[c] Laboratory of Adsorption and Catalysis, Department of Analytical and Physical Chemistry, Campus do Pici, Federal University of Ceara, Fortaleza-CE 60020-181, Brazil
[d] Centro de Investigação de Montanha (CIMO), Instituto Politécnico de Bragança, Campus de Santa Apolónia, 5300-253 Bragança, Portugal
[e] Laboratório Associado para a Sustentabilidade e Tecnologia em Regiões de Montanha (SusTEC), Instituto Politécnico de Bragança, Campus de Santa Apolónia, 5300-253 Bragança, Portugal

ARTICLE INFO

Keywords:
Adsorption
Sustainability
TEA
Biogas upgrading

ABSTRACT

This study presents an integrated approach in biogas upgrading technology through the development and optimization of a shaped MIL-160(Al)-based pressure/vacuum swing adsorption (PSA/VPSA) system. Combining detailed experimental investigations with comprehensive process modeling and techno-economic analysis, we demonstrate a complete pathway from fundamental dynamic adsorption to industrial implementation. Breakthrough tests reveal notable CO_2/CH_2 separation performance with shaped MIL-160(Al), while 23 cyclic PSA experiments achieved over 90 % methane purity. Advanced process modeling, validated with less than 5 % deviation from experimental data, enables successful scale-up to industrial VPSA configurations, where 38 distinct cases were evaluated to identify an optimal system producing 99.81 % pipeline-quality biomethane with 92.6 % recovery. Our holistic techno-economic assessment reveals the system's acceptable economic viability, with the total capital expenditure (CapEx) of $14.33 million. Accordingly, this work provides clear methodological insights that strengthen the understanding of MIL-160(Al)-based PSA/VPSA process and support its potential application for biogas upgrading.

1. Introduction

Growing concerns over fossil fuel depletion, escalating greenhouse gas emissions, and the intensifying impacts of climate change have brought renewed focus to the development and implementation of sustainable and renewable energy technologies [1,2]. Within this landscape, biogas has gained significant traction as a viable alternative energy carrier, supported by a steady rise in global production [3,4]. On the other hand, raw biogas contains substantial amounts of CO_2 and other trace impurities, which lower its energy content and limit its direct use [5]. Therefore, biogas upgrading - primarily through CO_2/CH_4 separation - is essential for producing high-purity biomethane suitable for grid injection, transportation fuels, or industrial applications [6]. Beyond improving fuel quality, the upgrading process also enables the capture of a concentrated CO_2 stream, further enhancing the environmental value of biogas systems [3,7]. To achieve this, various technologies have been developed for biogas upgrading, which detailed information about these processes are provided in Supporting Information. Among various technologies, PSA is particularly attractive due to its favorable energy consumption profile, lower capital and operating costs, high productivity, ease of maintenance, and environmental compatibility [8].

In recent years, significant efforts have been devoted to enhancing the performance of PSA and Vacuum PSA (VPSA) processes for biogas upgrading, either by exploring diverse classes of adsorbents to improve CO_2/CH_4 separation efficiency or by designing and developing

* Corresponding author at: Laboratory of Separation and Reaction Engineering (LSRE), Associate Laboratory LSRE/LCM, Faculty of Engineering, University of Porto, Rua Dr. Roberto Frias, 4200-465 Porto, Portugal.
E-mail address: mohsen.karimi@fe.up.pt (M. Karimi).

https://doi.org/10.1016/j.seppur.2025.136571
Received 25 October 2025; Received in revised form 12 December 2025; Accepted 18 December 2025
Available online 19 December 2025

optimized process configurations to maximize overall upgrading efficiency. It is worth noting that in PSA cycles with pressure equalization, CH_4 recovery over 90 % and purity over 95 % is achievable, while VPSA process has a potential to reduce the energy consumption by 20–30 % compared to the PSA [9,10].

The efficiency of separation in cyclic adsorption processes strongly depends on both the type of adsorbent and the configuration of the adsorption cycle [11,12]. Nevertheless, due to the multitude of influencing parameters, identifying optimal operating conditions to meet specific separation targets remains a significant challenge [11]. Moreover, given the inherent complexity of cyclic adsorption systems - such as PSA, VPSA, and TSA – there is a lack of available experimental data for MOF materials in cyclic process applications for CO_2 separation and sequestration [11]. Consequently, only a limited number of experimental studies have been reported in the literature addressing this issue [12].

Nonetheless, Metal-Organic Frameworks (MOFs), a relatively recent class of porous crystalline materials, have attracted substantial attention in gas separation due to their tunable pore structures, chemical functionalities, and wide compositional variety [13]. Several studies highlight their performance in carbon capture and gas purification, noting their versatility in terms of selectivity, adsorption thermodynamics, and kinetics [14]. Although early MOFs were hindered by poor thermal/chemical stability, high production costs, and limited forms (mainly powders) [13], recent advancements have addressed these challenges [13,14]. Building upon this progress, MIL-160(Al) - a bio-derived, Al-based MOF synthesized from Furane Dicarboxylic Acid (FDCA) - has been introduced as a promising candidate [15]. Its favorable adsorption capacity, selectivity, and manageable heat of adsorption underscore its suitability for biogas upgrading applications [16]. Accordingly, in this study, MIL-160(Al) has been selected for biogas upgrading.

1.1. Techno-economic assessment (TEA)

The primary goal of chemical processes is to generate profit, making an understanding of process economics essential in process design. Process economics serves three key functions in this context including assessing design alternatives, optimizing the process, and evaluating project profitability [17]. Cost analysis is necessary to compare different design choices, such as which carbon mitigation process is more suitable financially. Certain process variables may significantly impact flowsheet development and overall profitability. These variables must be optimized to enhance efficiency. Also, the financial viability of the entire project should be assessed at various design stages to determine whether it remains economically feasible [17]. In this context, TEA is employed as an efficient tool to evaluate that technology financially. In this study, the final annualized cost (FAC) is estimated by considering both the capital expenditure (CapEx) and the operating expenditure (OpEx). More descriptions can be found in Supporting Information.

1.2. Research objectives

In pursuing studies aimed at improving and evaluating the performance of (V)PSA processes for biogas upgrading, we conducted a comprehensive investigation by addressing the following key aspects:

I. Based on a developed dynamic adsorption equilibrium measurement system, a lab-scale PSA unit was designed for biogas upgrading using shaped form MIL-160(Al). To accurately assess the effects of rinse and purge flowrates on process performance, 23 distinct PSA experiments were conducted, and the yield from each run was evaluated. Furthermore, the experimental results were validated through process simulation, with a focus on the best-performing conditions.
II. In the subsequent phase, an industrial-scale VPSA process was developed for biogas upgrading. Following a similar strategy, 38 different VPSA configurations were analyzed by calculating and reporting key performance indicators (KPIs), including CH_4 purity, CH_4 recovery, productivity, and energy consumption. This allowed for a detailed understanding of the influence of rinse and purge flowrates on the process at an industrial scale.
III. Finally, a techno-economic assessment (TEA) was carried out by estimating both capital and operating costs associated with the VPSA system. The analysis included the evaluation of equipment sizing, electricity consumption, and auxiliary systems. Besides, sensitivity analyses were performed to examine the impact of key operational parameters – such as MOF price and replacement period, electricity price, and plant lifetime - on overall process economics. This comprehensive TEA offers valuable insight into the financial feasibility of MIL-160(Al)-based VPSA for large-scale biogas upgrading.

2. Materials and methods

2.1. Materials and instrumentation

As already mentioned, in this work the shaped form MOF MIL-160 (Al) was selected for biogas upgrading, which the detailed information regarding the synthesis, shaping protocol and all specifications can be found in [15]. Furthermore, N_2 adsorption-desorption isotherm at 77 K is represented in Fig. S1 (Supporting Information), also some of the key characteristics are illustrated in Table 1 [16]. The studied gases such as carbon dioxide (99.99 %) and methane (99.95 %) and the required inert gas, helium (99.999 %), were provided by Air Liquide.

In the present study, both dynamic breakthrough and cyclic adsorption experiments were performed using a custom-built fixed-bed setup designed with dual columns. For the current investigation, only one adsorption column was utilized to mimic counter-current operation while simplifying process control. The inlet gas flowrates were precisely regulated using high-accuracy mass flow controllers, and the outlet flowrate was simultaneously monitored using a mass flow meter, all instruments calibrated and supplied by Alicat Scientific. The outlet gas composition was continuously tracked via an in-line infrared gas analyzer to evaluate separation performance in real time. To monitor thermal behavior, a thermocouple was positioned at the axial center of the bed. System pressure was maintained at the desired level using a backpressure regulator obtained from Bronkhorst. The detailed specifications of the setup and corresponding operational parameters are listed in Table 1, in addition more details can be found elsewhere [16].

Table 1
The characteristics of studied adsorbent (Al-based MOF MIL-160) accompanied with the specifications of fixed-bed adsorption set-up [16].

Adsorbent properties[1]	
Parameter	Numerical values
Particle radius,	1.35×10^{-3} (m)
Bulk density at 0.0037 MPa	1.07 (g/cm^3)
Median pore diameter (volume) at 7.7 MPa and 0.1 cm^3/g	0.162 (μm)
Median pore diameter (area) at 119.8 MPa and 9.7 m^2/g	0.0104 (μm)
Average pore diameter (4 V/A)	0.0454 (μm)
Apparent (skeletal) density at 206.5 MPa	1.40 (g/cm^3)
Total intrusion volume	0.22 (cm^3/g)
Total pore area	19.45 (m^2/g)
Micropore volume	0.336 (cm^3/g)
The specifications of fixed-bed adsorption set-up	
Bed length	6.8 (cm)
Bed diameter	2.1 (cm)
Bulk bed density	463.03 (kg/m^3)
Mass of sample	10.9 (g)
Intraparticle porosity	0.31 (m^3 $_{void}$/m^3 $_{bead}$)
Interparticle or bed porosity	0.48 (m^3 $_{void}$/m^3 $_{bed}$)

2.2. Experimental procedures

In this study, the dynamic breakthrough experiments and PSA cycles were conducted using the same fixed-bed experimental setup, as previously described. Prior to testing, the fresh MIL-160(Al) samples underwent an activation procedure by purging the column with helium at a flow rate of 327.5 NmL/min, while the temperature was increased at a rate of 1 K/min up to 423 K and maintained overnight to ensure complete desorption of moisture and volatile species. To characterize the adsorption dynamics and provide a basis for process modeling, two breakthrough experiments were carried out under controlled conditions, which detailed description of performed experiments have been discussed in the Supporting Information (Appendix A). Subsequently, a five-step PSA process with one column was developed and operated at 318 K and 4.5 bar, with the sequence comprising counter-current pressurization with methane, a feed step, a rinse step with pure CO_2 to enhance product purity, a blowdown to near-atmospheric pressure, and a counter-current purge with methane for bed regeneration [9,12]. The full operational parameters for the PSA experiments are summarized in Table 2.

3. Theory and methods

3.1. Mathematical model

To accurately simulate and optimize the performance of pressure swing adsorption (PSA) systems, a reliable mathematical framework describing adsorption equilibria and transport phenomena is essential. The Langmuir model was adopted in this study (see Appendix D, Table S3), given its effectiveness in representing multicomponent gas adsorption behavior [18]. This approach and the corresponding parameters [18,19], which have been considered in this study are described in Supporting Information.

To capture the transient nature of mass transfer within the packed bed, a dynamic model incorporating mass, momentum, and energy conservation equations was developed. This formulation includes several assumptions to ensure numerical tractability without compromising physical accuracy, such as: (i) the gas phase follows ideal gas behavior, (ii) plug flow with axial dispersion, (iii) mass transfer into the particle is governed by a lumped kinetic resistance model described according to Linear Driving Force approach, (iv) heat transfer is treated under non-isothermal, non-adiabatic conditions with no internal conduction, (v) thermal equilibrium between the solid and fluid phases, (vi) constant void and bed density along the column, (vii) no mass, heat or velocity gradients in the radial direction, (viii) the Ergun equation is utilized for pressure drop estimation across the bed, and (ix) axial dispersion is incorporated via the Langer correlation [20]. A full description of the governing equations and associated constitutive relations is provided in Appendix D (Supporting Information).

Subsequent to equilibrium characterization, the PSA process was numerically implemented under experimentally inspired conditions using appropriate boundary settings (see Table S4, Appendix D). Furthermore, the specifications and characteristics of designed VPSA process for biogas upgrading in the industrial scale are described in Table 3. The model performance was assessed through key indicators - methane purity, recovery, productivity, and energy consumption - as defined by Eqs. (1)–(5) [21,22]. These metrics collectively quantify the efficiency and viability of the process under various operating scenarios.

$$CH_4 purity(\%) = \frac{\sum_j \left(\int_0^{t_j} F_{CH_4,out} dt \right)}{\sum_j \left(\int_0^{t_j} F_{CH_4,out} dt + \int_0^{t_j} F_{CO_2,out} dt \right)} \times 100 \quad (1)$$

$$CH_4 rec(\%) = \frac{\sum_j \left(\int_0^{t_j} F_{CH_4,out} dt \right) - \sum_k \left(\int_0^{t_k} F_{CH_4,in} dt \right)}{\sum_l \left(\int_0^{t_l} F_{CH_4,in} dt \right)} \times 100 \quad (2)$$

$$CO_2 purity(\%) = \frac{\sum_m \left(\int_0^{t_m} F_{CO_2,out} dt \right)}{\sum_m \left(\int_0^{t_m} F_{CH_4,out} dt + \int_0^{t_m} F_{CO_2,out} dt \right)} \times 100 \quad (3)$$

$$CO_2 rec(\%) = \frac{\sum_m \left(\int_0^{t_m} F_{CO_2,out} dt \right) - \sum_m \left(\int_0^{t} F_{CO_2,in} dt \right)}{\sum_l \left(\int_0^{t_l} F_{CO_2,in} dt \right)} \times 100 \quad (4)$$

$$CH_4 productivity\left(mol kg^{-1} h^{-1}\right) = \frac{\sum_j \left(\int_0^{t_j} F_{CH_4,out} dt \right) - \sum_k \left(\int_0^{t_k} F_{CH_4,in} dt \right)}{mass of dry adsorbent \times t_{cycle}} \quad (5)$$

Here, for CH_4 purity calculation, j denotes the feed and rinse steps. It also can be found in Eqs. (2) and (5), for CH_4 Recovery and Productivity calculations. The use of the subscripts in those equations denotes multiple steps of the PSA cycle and allows the equations to remain compact. In Eq. (2), k denotes the purge and pressurization steps, and l is the feed and pressurization steps. For CO_2 purity calculation, in Eq. (3), m denotes the blowdown and purge steps. For CO_2 recovery (Eq. (4)), RIN denotes the rinse step and l is the same used in Eq. (2). A schematic diagram of the PSA cycle can be found in Fig. S6 (Supporting Information). Furthermore, the energy consumption through the compressor and vacuum pump is estimated using Eq. (6) [19], by assuming the efficiency of 80 % for compressor and 60 % for vacuum pump:

$$Energy consumption = \frac{1}{\eta} \dot{n} R_g T_g \frac{\gamma}{\gamma - 1} \left(\left(\frac{P_H}{P_L} \right)^{\frac{\gamma - 1}{\gamma}} - 1 \right) \quad (6)$$

here, $\dot{n}$ is the molar flow rate, $R_g$is the ideal gas constant, T_g the gas temperature, $\eta$is the pump efficiency, and $\gamma$is the specific heat ratio of the gas $\left(\gamma = \frac{C_P}{C_V} \right)$, as well P_L and P_H indicate the lower and higher pressure, respectively. Finally, the numerical solution of the resulting partial differential equation system was carried out using the gPROMS modeling environment, employing a second-order orthogonal collocation method discretized over 28 finite elements to ensure both stability and resolution.

Finally, a multi-objective optimization strategy was applied to discrete process data to simultaneously evaluate CH_4 purity, CH_4 recovery, and energy consumption. To ensure comparability and balanced contribution of each objective, a normalization technique was employed prior to constructing a weighted aggregate objective function. This formulation enabled the conversion of a multi-criteria problem into a single-objective framework, facilitating computational efficiency without compromising the integrity of the performance evaluation. The

Table 2
Determined cycles to separate CO_2/CH_4 at the lab scale cyclic set-up with one column.

PSA steps	PSA variables					
	The studied compositions		Flowrate (mL/min)	Step time (s)	Temperature (K)	Pressure (bar)
	CO_2%	CH_4%				
Pressurization	–	100	400	50	318	1 → 4.5
Feed	40	60	700	300	318	4.5
Rinse	100	0	270	350	318	4.5
Blowdown	–	–	–	50		4.5 → 1.0
Purge	–	100	142	60		1.0

Table 3
The specifications and characteristics of designed VPSA process with one column for biogas upgrading on the industrial scale.

The bed specifications of industrial VPSA process	
Parameter	Numerical values
Bed volume	12.37 (m^3)
Bed diameter	1.5 (m)
Bed height	7.0 (m)
Bed area	1.77 (m^2)
Bed porosity	0.487 (−)
Particle radius	1.35×10^{-3} (m)
Bulk bed density	463.03 ($kg.m^{-3}$)

PSA steps	PSA variables					
	The studied compositions		Flowrate (L/min)	Step time (s)	Temperature (K)	Pressure (bar)
	CO_2%	CH_4%				
Pressurization	–	100*	35×10^3	230	318	0.2 → 4.5
Feed	40	60	100×10^3	170	318	4.5
Rinse	100*	0	22.5×10^3-74×10^3	100	318	4.5
Blowdown	–	–	0	75		4.5 → 0.2
Purge	–	100*	1×10^3-10×10^3	340		1.0 → 0.2

* The Pressurization and Purge compositions were according to the Feed out composition, the Rinse composition was according to the blowdown and purge out composition. So, it is not a fixed number, nor 100 % of CH_4.

weighting structure embedded within the objective function allowed for prioritization based on specific process requirements. The optimization algorithm systematically explored the discrete solution space and successfully identified process configurations that achieved an optimal trade-off among the three competing performance metrics, demonstrating the method's effectiveness for complex engineering systems with inherent performance conflicts.

3.2. Techno-economic assessment (TEA)

In the present study, the capital expenditure (CapEx) is presented based on 2024 price levels, with older cost estimates adjusted to 2024 values using the average Chemical Engineering Plant Cost Index (CEPCI) (Eq. (7)) [23,24].

$$\frac{CEPCI_1}{CEPCI_2} = \frac{CapEx_1}{CapEx_2} \tag{7}$$

In Eq. (7), $CEPCI_1$ and $CEPCI_2$ represent the CEPCI factor in the years 1 and 2, respectively. Also, $CapEx_1$ is the capital cost in year 1 and $CapEx_2$ shows the capital cost in the year 2. It is worth mentioning that the equipment costs are estimated by the ASPEN Economic Analyzer module. In this context, the major equipment designed in this process are a drum, a compressor and a vacuum pump. The free on-board cost (FOB) estimated by ASPEN Economic Analyzer is depicted in Table S2 (Supporting Information). The delivery purchased cost (DPC), which is the base of the following calculations is estimated by addition of 10 % of FOB cost as the freight [17].

The DPC of this flowsheet at 2023 is 1663420 $, which will be 1,668,215 $ in May 2024 according to Eq. (7) and employing the CEPCI of 2023 (797.9) and May 2024 (800.2) (CEPCI). The CapEx consists of three parameters including direct cost (DC), indirect cost (IC), and interest during construction [17,25,26]. Indeed, the direct cost, which is defined as all operational costs in the field to procure and install the equipment, is sum of the costs of the following activities mentioned in Table 4 [17,26,27]. In this way, the direct cost (DC) is determined around $6.7 \times 10^6$$ according to the data reported in Table 4. On the other hand, the indirect cost follows a similar procedure [17,26,27]. From the reported data in Table 4, the indirect cost (IC) is calculated $7.5 \times 10^6$$.

Finally, the interest during construction period is determined by the following correlation [28]:

$$Interest = Interestrate \times 2.02 \times DPC \tag{8}$$

Table 4
The calculated direct and indirect costs in the developed approach.

Direct cost calculation		
Activities	Multiplier	Cost ($)
Delivered purchased cost (DPC)	–	1.6×10^6
Installation	0.43 DPC	0.7×10^6
Piping	0.66 DPC	1.1×10^6
Instrumentation & control	0.4 DPC	6.6×10^5
Insulation	0.03 DPC	5.0×10^4
Electrical systems	0.1 DPC	1.67×10^5
Buildings	0.47 DPC	7.84×10^5
Yard improvement	0.2 DPC	3.34×10^5
Utilities	0.5 DPC	8.34×10^5
Off-site	0.2 DPC	3.34×10^5
Land	0.08 DPC	1.33×10^5
Indirect cost calculation		
Activities	**Multiplier**	**Cost ($)**
Design & engineering	0.25 DC	1.69×10^6
Construction	0.35 DC	2.37×10^6
Contractor's fee	0.08 DC	5.43×10^5
Contingency	0.40 DC	2.72×10^6
Start-up	0.03 DC	2.04×10^5

* DPC: Delivery Purchased Cost.
** DC: Direct Cost.

$$AnnualizedCost = CapEx \times \frac{j(1+j)^n}{(1+j)^n - 1} \tag{9}$$

The interest rate is considered 5 % [28], consequently from the above equation, the interest is calculated 168,489.71 $. Eventually, from the data mentioned in this subsection, the CapEx is 14,327.81 k$. To make the CapEx comparable with other parameters in TEA approach, we need to reveal the CapEx in a time period; as a result, Eq. 9 is applied to include the CapEx with plant lifetime (n) and the interest rate (j) [23].

In this study, the plant lifetime and interest rate are considered as 15 years and 5 %, respectively [28]. In this context, the annualized CapEx is calculated 1380.37 k$/y. To evaluate the impact of plant lifetime on the plant FAC, a sensitivity analysis was implemented on plant lifetime (see section 4.3.3). On the other hand, operating expenditure (OpEx) includes both fixed operating cost (FOC) and variable operating costs (VOC). FOC covers expenses such as labor, maintenance, taxes, insurance, overhead and financial working capital (Table 5). Labor costs are estimated based on a rate of $34.50 per person hour. VOC accounts for

Table 5
A summary of key estimated fixed and variable operating costs.

Parameter		Multiplier	Cost (k$/y)
Variable operating cost (VOC)	**Electricity**	–	**Related to conditions**
	Adsorbent replacement	–	179
Fixed operating cost (FOC)	Labor	–	554
	Maintenance	0.07 DPC	114
	Taxes & insurance	0.03 DC	57
	Overhead	0.017 DC	28
	Financial working capital	0.09 * 1/12 variable operating cost	Related to VOC

costs related to adsorbent replacement and electricity (Table 5). Electricity cost is calculated by multiplying the total electricity consumption of the CO_2 capture process by the unit costs listed in (Table 6). For adsorbent replacement cost calculation, it is assumed the job is implemented in one day with two operators and also, 20 % is added as transportation.

In line with literature review [29,30], the cost of metal-organic framework (MOF) was assumed to be $55 per kg, with a replacement cycle of 1.5 years [29,30]. Given the uncertainty in estimating both the cost and lifespan of MOFs, a sensitivity analysis was performed to assess the impact of these variables on the final annualized cost (FAC) of the designed plant in section 4.3.3.

4. Results and discussion

4.1. Lab scale adsorption experiments

In this study, to have a precise knowledge on the dynamic of system and also to validate the developed model, firstly, two breakthrough experiments were conducted, which to reduce the size of the paper, as much as possible, the related results and also the detailed description have been presented in Appendix A. Afterwards, relying on dynamic outcomes, 23 lab-scale PSA experiments were designed to evaluate the performance of shaped MOF MIL-160(Al) in a PSA system for biogas upgrading, with a focus on optimizing rinse and purge flowrates to maximize methane purity while minimizing energy consumption. All performed experiments accompanied by detailed specifications have been reported in Appendix C.

The lab-scale investigation systematically evaluated the performance of shaped MIL-160(Al) through breakthrough experiments and PSA cycling, with key findings illustrated in Figs. 1–3. Fig. 1 presents the critical relationship between process parameters and separation performance, revealing fundamental insights into the system's behavior. The purge flowrate optimization (Fig. 1a) demonstrates a clear maximum in methane purity (90.26 %) at 150 mL/min, beyond which excessive methane loss reduces recovery (for instance methane purity of 92.2 % at 250 mL/min). This optimum reflects the balance between complete CO_2 desorption and minimizing product gas displacement, with the corresponding energy consumption (Fig. 1b) showing the expected trade-off between purity and process efficiency. It is worth noting that concerning the low flowrates of lab-scale experiments, there is not a meaningful difference in energy consumption on such scale. Moreover, the rinse step analysis (Fig. 1c-d) provides equally important insights, where the 40 and 260 mL/min represent the highest (90.3 %) and lowest (61.5 %) methane purity, respectively. The distinct power-law relationship in Fig. 1d confirms the expected flowrate dependence of energy consumption, with the exponent value indicating significant viscous losses in the packed bed. These experimental optimizations directly informed the cycle parameters used in subsequent validation studies. Fig. 2 extends this analysis through contour plots that visualize the complex interactions between rinse and purge flowrates. The purity surface (Fig. 2a) reveals a broad operational plateau where methane purity exceeds 96 %, centered around the experimentally determined optima from Fig. 1. The corresponding energy consumption landscape (Fig. 2b) shows steeper gradients at higher flowrates, emphasizing the increasing energy penalty for marginal purity gains beyond the optimal region.

Table 6
A summary of considered constants and assumptions in estimating OpEx.

Parameter	Quantity
Electricity price in Portugal at 2024	0.12 $/kWh
Labor salary	34.5 $/person.h
Number of operators	2 people
Working shift	4
MOF unit price	55 $/kg
MOF replacement period	1.5 y
Bed porosity	0.487
Bed bulk density	463 kg/m^3

The experimental validation in Fig. 3 provides critical confirmation of the process model's accuracy. The pressure profiles (Fig. 3a) capture the characteristic blowdown behavior - an initial rapid pressure drop (4.5 → 1.0 bar in 40 s) as gas evacuates from the column, followed by purge flow (1.0 bar in 60 s). The temperature dynamics (Fig. 3b) quantitatively match the predicted exotherm, with the observed thermal wave propagation velocity confirming the bed's limited heat transfer characteristics. Flowrate measurements (Fig. 3c) during cyclic steady-state operation show acceptable agreement (±5 %) with model predictions, particularly during the critical rinse step where displacement efficiency is paramount.

These comprehensive experimental results, supported by rigorous model validation, establish MIL-160(Al) as a technically viable adsorbent for biogas upgrading. The clear optimization pathways revealed in Figs. 1–2, combined with the accurate process representation demonstrated in Fig. 3, provide a solid foundation for industrial-scale implementation. The lab-scale data particularly highlights the importance of balancing purity targets with energy consumption, while the excellent model agreement gives confidence in predictive scale-up capabilities.

4.2. Industrial VPSA for biogas upgrading

4.2.1. Effect of purge flowrate on separation performance

The industrial-scale VPSA process demonstrated a strong dependence on purge flowrate for achieving optimal methane purity and energy efficiency. As shown in Fig. 4a, increasing the purge flowrate from 1.5×10^3 to 10^4 L/min improved methane purity from 80.93 % to 98.96 %, primarily due to enhanced desorption of CO_2 from the MIL-160(Al) adsorbent. This improvement can be attributed to the higher purge flowrates creating a stronger convective flow through the adsorbent bed, reducing mass transfer limitations and improving the removal of CO_2 from the adsorbent's micropores (0.336 cm^3/g, Table 1), where, in this case, the adsorption occurrence dominates. This is particularly important for MIL-160(Al), which exhibits a moderate CO_2 adsorption capacity [16] and benefits from efficient regeneration. At purge flowrates above 5×10^3 L/min, methane purity reached a plateau (Fig. 4a), indicating that the adsorbent was regenerated and that further increasing in purge flowrate could not provide additional improvement. However, energy consumption increased significantly (Fig. 4b) since higher flowrates increase the amount of gas that must be removed from the bed. The rise in energy consumption (Fig. 4b) reflects the increased work required by the vacuum pump (to achieve <0.2 bar during regeneration). Thus, the optimal purge flowrate of 8×10^3 L/min represents a balance between purity (99.81 %) and energy efficiency (954.23 kWh), aligning with industrial benchmarks for biogas upgrading [31].

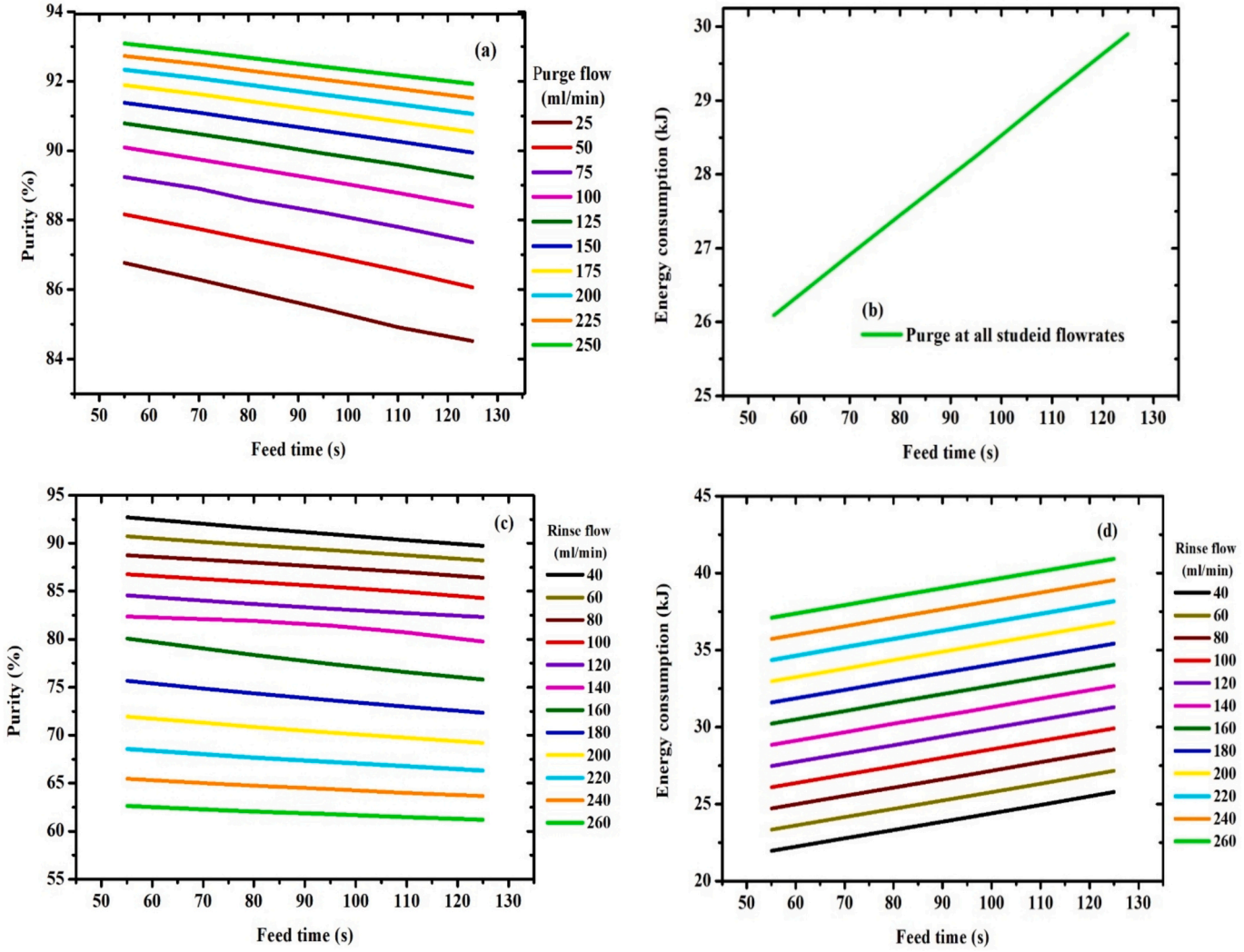

Fig. 1. The impact of different purge flowrates in the lab-scale on (a) the purity of methane and (b) the energy consumption, as well as the impact of different rinse flowrates in the lab-scale on (c) the purity of methane and (d) the energy consumption.

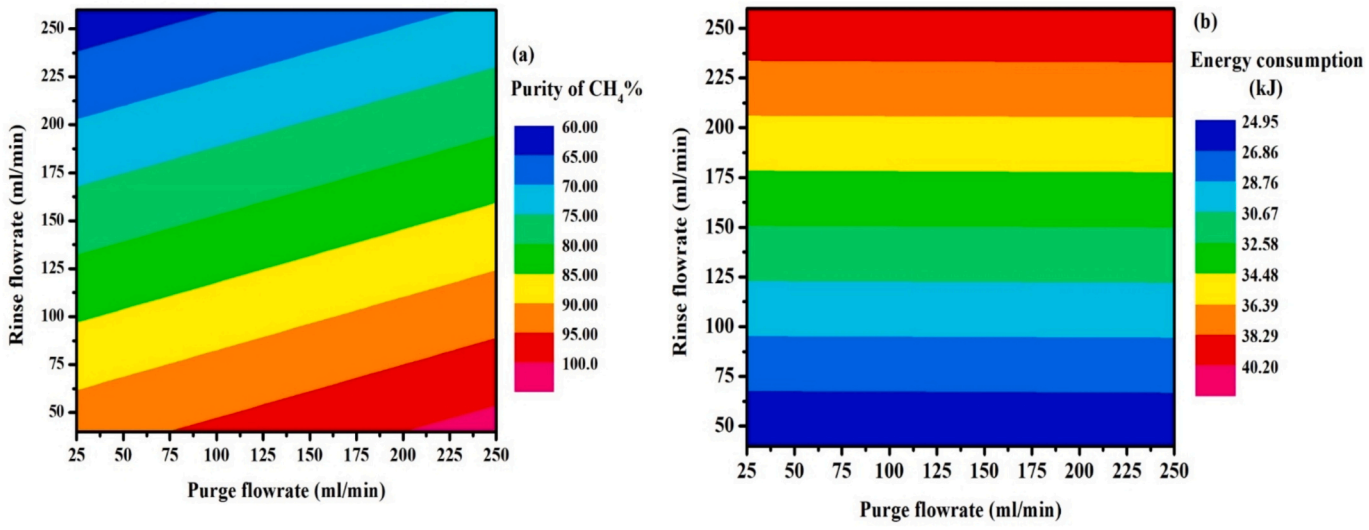

Fig. 2. Counter graphs of (a) the purity of methane and (b) the energy consumption as a function of rinse and purge flowrates (feeding time: 110 s).

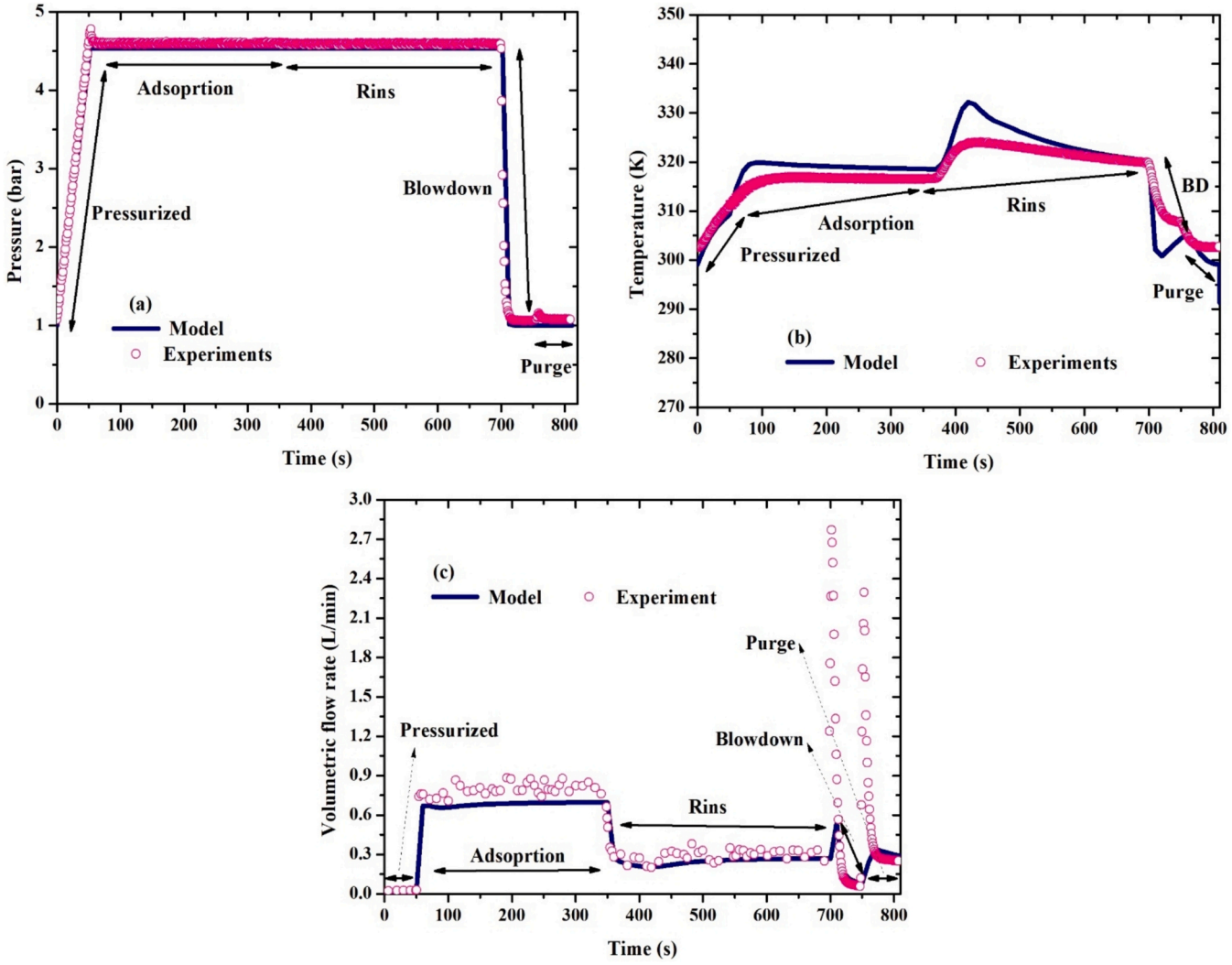

Fig. 3. The experimental and modeling results: (a) pressure (b) temperature history and (c) total volumetric flowrate of the best accomplished PSA experiment in the lab-scale.

4.2.2. Role of rinse flowrate in process optimization

The rinse step, which utilizes pure CO_2 to displace residual impurities, is critical for achieving high methane purity in the product stream. Fig. 4c shows that a rinse flowrate of 22.5 × 10^3 L/min maximized methane purity (99.96 %) by ensuring complete displacement of adsorbed CO_2 from the bed. Higher flowrate than 60 × 10^3 L/min, the rinse front did not fully traverse the bed, leaving behind CO_2-rich zones that reduced purity. It is worth noting that above 70 × 10^3 L/min, excessive rinse flow led to methane dilution and significant energy consumption (Fig. 4d). The energy penalty associated with higher rinse flowrates can be explained by:

1. Compressor Work: The energy required to compress the CO_2 recycle stream scales linearly with flowrate, as described by the adiabatic compression equation (Eq. (6)).
2. Pressure Drop: The Ergun equation (Table S3) predicts a quadratic increase in pressure drop with flowrate, further elevating energy demands.

Notably, the rinse step's efficiency is also influenced by the adsorbent's kinetic properties. MIL-160(Al)'s rapid CO_2 adsorption/desorption kinetics [16] enabled shorter rinse times (100 s, Table 4) compared to traditional zeolites [32], contributing to the process's overall productivity.

4.2.3. Key performance indicators (KPIs) in process optimization

The industrial VPSA system's performance was evaluated using four KPIs (Fig. 5):

Methane Purity (Fig. 5a): The contour plot reveals a broad operational window (>95 % purity) for rinse flowrates of 22 × 10^3–50 × 10^3 L/min and purge flowrates of 4.5 × 10^3–10 × 10^3 L/min. This robustness is attributed to MIL-160(Al)'s high CO_2/CH_4 selectivity [16] and the VPSA cycle's efficient regeneration.

CH_4 Recovery (Fig. 5b): Peak recovery occurred at moderate purge flowrates, where CO_2 desorption was maximized without excessive methane loss. The recovery profile mirrors the purity trends, underscoring the trade-off between these metrics.

Productivity (Fig. 5c): The highest productivity was achieved at the highest rinse flow and the lowest purge flow, demonstrating the importance of balancing rinse intensity with cycle time. This value surpasses conventional PSA systems using zeolites 13×, as one of the benchmark adsorbents for biogas upgrading [32], highlighting MIL-160 (Al)'s industrial potential.

Energy Consumption (Fig. 5d): The energy minimum coincided with the optimal flowrate conditions, validating the process's scalability. The VPSA configuration's energy advantage over traditional PSA (20–30 % reduction [33–36] stems from the vacuum-assisted blowdown, which reduces the work required for CO_2 desorption.

On these grounds, the industrial-scale results demonstrate that MIL-

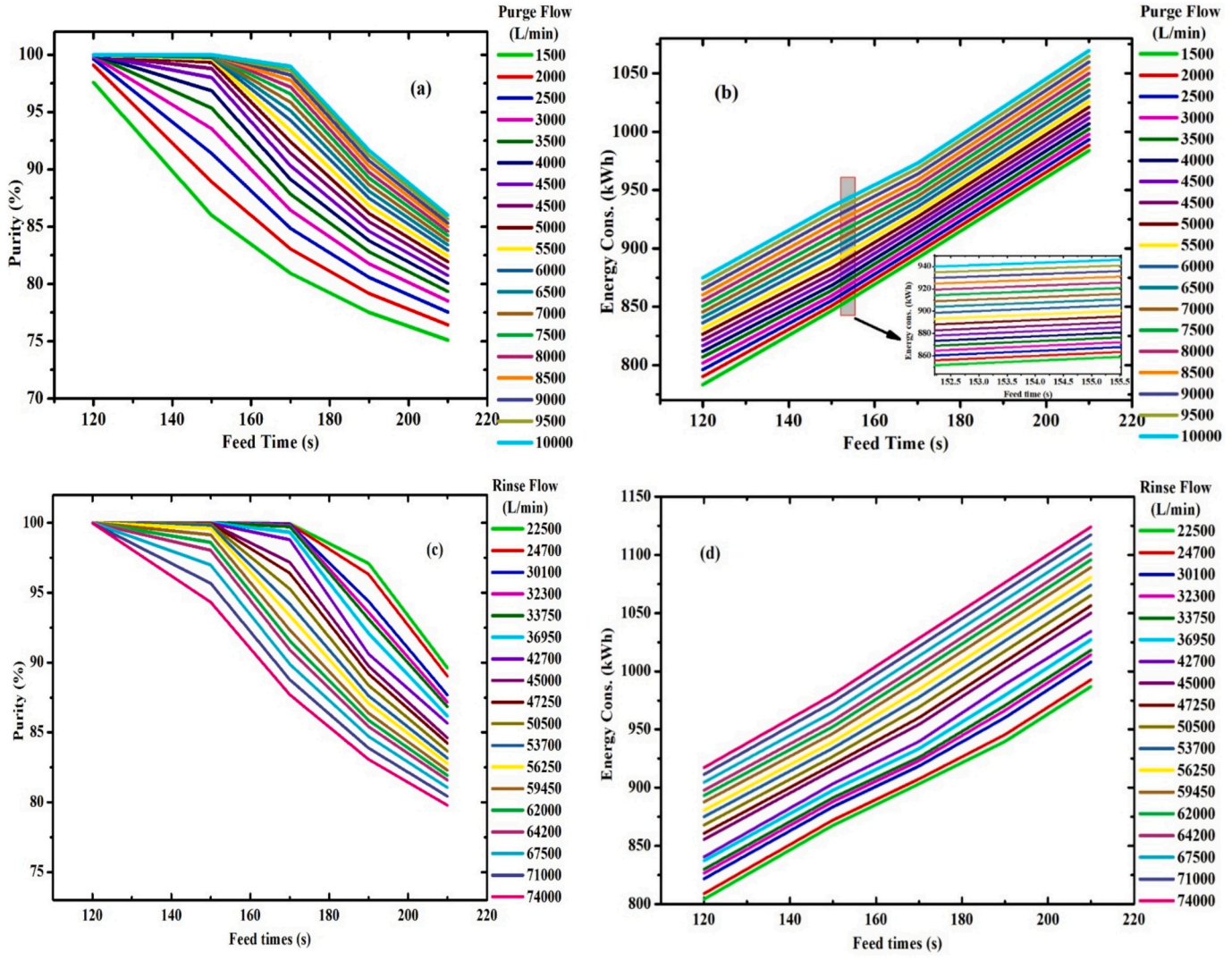

Fig. 4. The impact of different purge flowrates in the industrial scale on (a) the purity of methane and (b) the energy consumption, as well as the impact of different rinse flowrates in the industrial scale on (c) the purity of methane and (d) the energy consumption.

160(Al)-based VPSA can achieve performance metrics comparable to or better than existing technologies (e.g., amine scrubbing, membrane separation) while offering distinct advantages, including (I) adsorbent stability: MIL-160(Al)'s hydrothermal stability [15] eliminates the need for frequent adsorbent replacement, reducing operational costs (Table 5); (II) process flexibility: the broad optimal range for rinse/purge flowrates (Fig. 5a–d) allows for adaptable operation under varying biogas feed conditions (e.g., 40–60 % CO_2); (III) energy efficiency: The 834–1047 kWh energy consumption is competitive with state-of-the-art systems [33–36], making it viable for large-scale deployment. These findings align with the techno-economic assessment (Section 4.3), which confirms the process's financial feasibility at industrial scales.

4.3. Techno-economic assessment (TEA)

The techno-economic assessment provides critical insights into the financial viability and optimization potential of the MIL-160(Al)-based VPSA system for industrial biogas upgrading. The analysis integrates process performance data with detailed cost modeling to identify key economic drivers and evaluate competitiveness against conventional technologies. It is worth noting that all related data to the TEA in this study have been reported in Appendix E (Supporting Information) for interested readers.

4.3.1. Capital expenditure (CapEx) analysis

The capital costs for the industrial-scale VPSA system were evaluated using a bottom-up approach, considering both direct and indirect costs (see Table 5). The total CapEx of $14.33 million was dominated by construction cost ($2.38 million), followed by design and engineering ($ 1.70 million). DPC stands for the next highest one with $ 1.67 million, particularly the compressor systems, which accounted for 10.02 % of the total CapEx. The piping cost (7.7 %) and utilities (5.8 %) represented other significant investments of the total CapEx. In line with this it was indicated that CapEx is about 44 % of the FAC.

4.3.2. Operating expenditure (OpEx) breakdown

The variable operating costs (Table 5) were dominated by (1) electricity consumption: considering the Portugal's industrial electricity rate (0.12/kWh, Table 6), this translated to $0.038/$Nm^3$, representing 51.6 % of VOC, (2) adsorbent replacement: MIL-160(Al) replacement every 1.5 years (Table 6) cost $179 k/year [29,30], including: (I) Material cost: $55/kg × 3231.65 kg (bed inventory within 1 year) = $17.77 × 10^4; (II) Labor: 48 person-hours × $34.5/h /1.5 year = $1104 (within 1 year); (III) Transportation: 20 % surcharge = $221; (IV) The adsorbent's cycle stability reduced replacement frequency versus zeolites (typically 1-year cycles [12,31,35]).

Nonetheless, the fixed operating costs included:(I) Labor ($554 k/

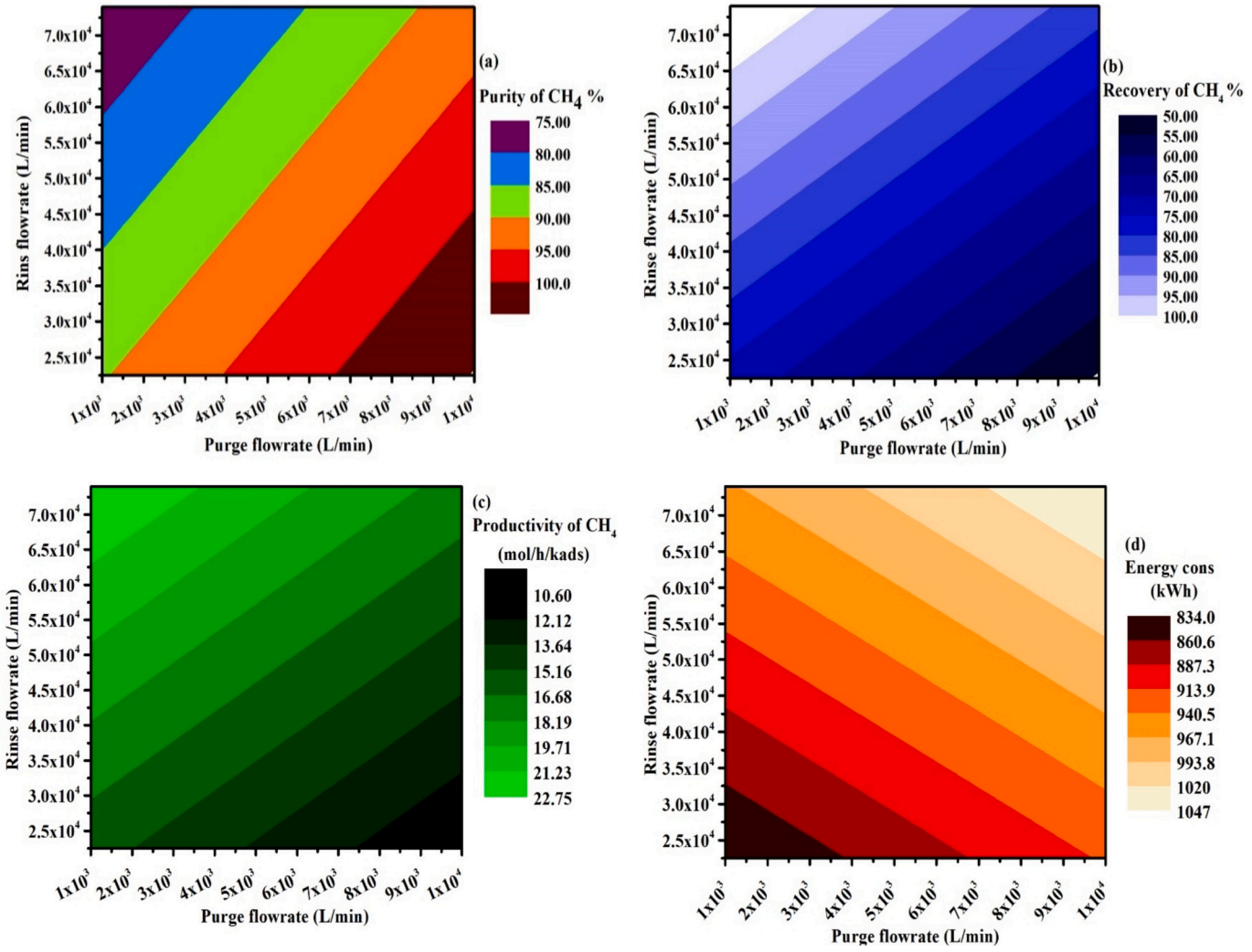

Fig. 5. Counter graphs of (a) the purity, (b) the recovery, (c) the productivity and, (d) the energy consumption of bio-methane as a function of rinse and purge flowrates (at the feeding time: 170 s).

year): continuous operation required 2 operators per shift × 4 shifts; (II) Maintenance (7 % of DPC = $114 k/year): Primarily for valve replacements and handling daily routine jobs at the plant.

4.3.3. *Sensitivity analysis and cost drivers*

The cost structure and operational parameters of the industrial-scale VPSA system through detailed analysis have been systematically illustrated in Figs. 6–8. A comprehensive analysis of how purge and rinse

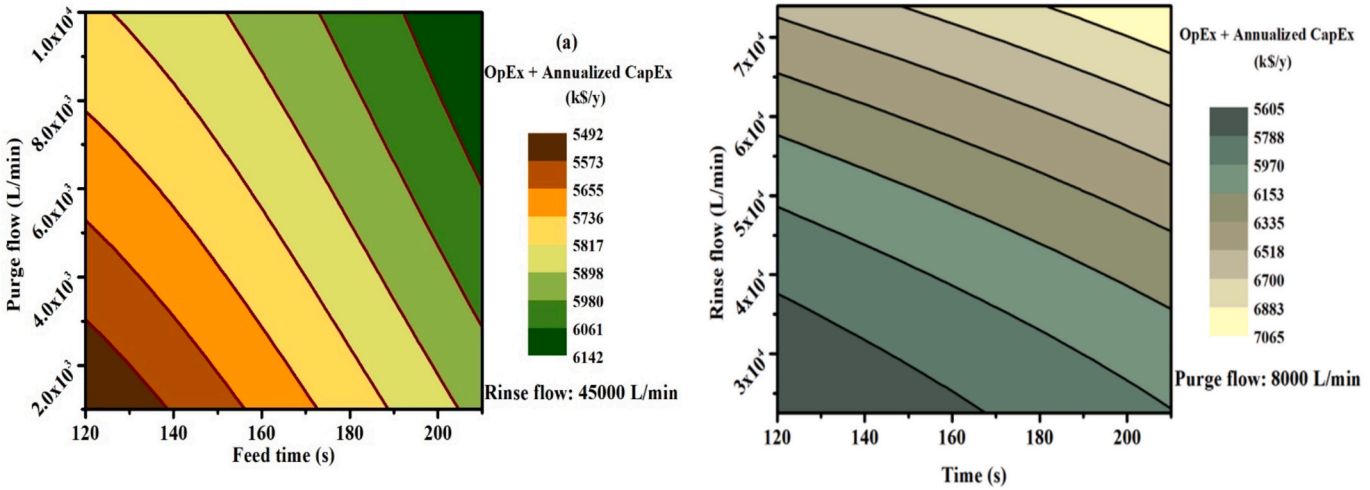

Fig. 6. An assessment on (a) purging flow impact on the FAC at different feeding time, (b) rinsing flow impact on the FAC and different feeding time.

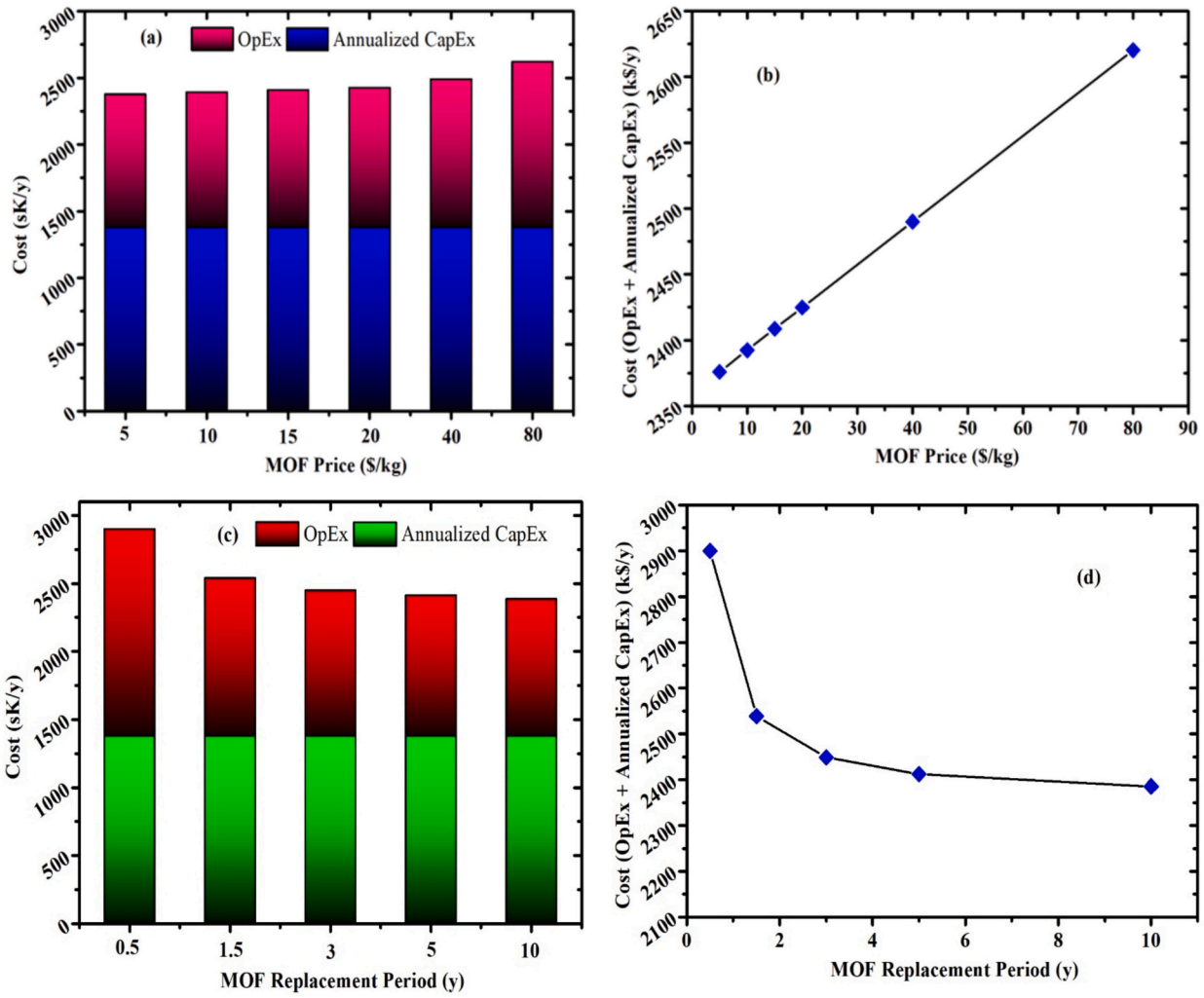

Fig. 7. MOF price impact on (a) OpEx and annualized CapEx, also(b) the FAC. The impact of MOF replacement period on (c) OpEx and annualized CapEx, also (d) the FAC.

flowrates influence the Final Annualized Cost (FAC) is demonstrated in Fig. 6. The contour plots demonstrate a distinct cost minimum at around 2×10^3 L/min purge flowrate (Fig. 6a) and 22.5×10^3 L/min rinse flowrate (Fig. 6b), corresponding to the optimal balance between methane purity (99.81 %) and energy consumption (903.3 kWh) shown in Figs. 4–5. The nonlinear cost increase beyond these flowrates reflects the cubic relationship between compressor power and flowrate (Eq. (6)), compounded by elevated pressure drops described by the Ergun equation.

The economic sensitivity to MIL-160(Al) adsorbent parameters is thoroughly explored in Fig. 7. Fig. 7a–b demonstrates how MOF unit price directly affects operating costs, with the current $55/kg price (Table 6) contributing $179 k/year to FAC (Table 6). Fig. 7c–d highlights the critical importance of adsorbent lifetime, where extending the replacement period from 1.5 to 3 years (through improved MOF stability) could reduce FAC by 3.6 %. These findings emphasize the need for ongoing developments in MOF manufacturing and stabilization techniques.

Fig. 8 completes the analysis with two crucial economic factors. Fig. 8a–b shows the linear relationship between electricity price and FAC, with each $0.01/kWh increase raising production costs by $18.5 k/y (Table 6). On the other hand, Fig. 8c–d evaluates plant lifetime effects, demonstrating that extending operation from 15 to 20 years decreases annualized CapEx by 16.7 % through improved capital recovery.

The TEA results, supported by the detailed cost breakdowns in Tables 5–6, position the MIL-160(Al)-based VPSA system as technologically and economically viable. The equipment-intensive nature of the process (54.4 % annualized CapEx share of FAC) is offset by its superior performance (99.81 % purity) compared to amine scrubbing [28,34,37], membrane systems [37,38], and also zeolite 13× [35,37] as one of the benchmark adsorbents for biogas upgrading. The clear visualization of cost sensitivities in Figs. 6–8 provides valuable guidance for both process optimization and future research directions, particularly in adsorbent development and energy recovery systems.

5. Conclusions

This study provides a detailed evaluation of a MIL-160(Al)-based biogas upgrading system, contributing to the understanding and optimization of its performance for sustainable energy applications. Our multiscale investigation, spanning adsorption to process design, yields several key findings. In this way, firstly, two breakthrough experiments were performed for CO_2 and CH_4 adsorption in a fixed bed column, in which the experimental results were successfully validated by the developed model. The 23 lab-scale PSA experiments were performed, that the KPIs were assessed for each one. The outcomes demonstrated that the CH_4 purity of 92.2 % is achievable using MIL-160(Al) for biogas upgrading. Afterwards, to have a better knowledge on the capacity of this adsorbent for commercial-scale application, 38 different VPSA configurations were developed by analyzing CH_4 purity, CH_4 recovery,

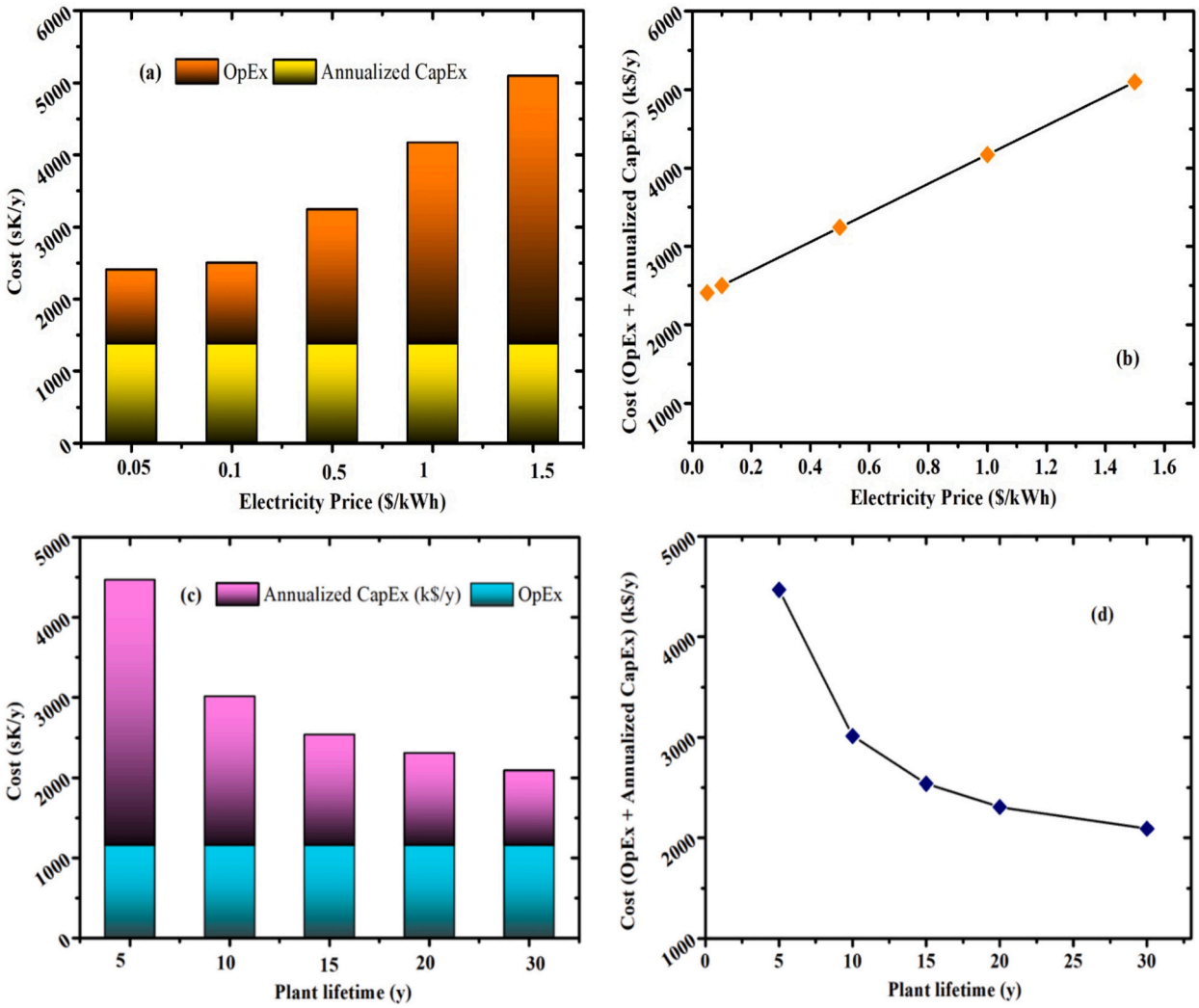

Fig. 8. Electricity price impact on (a) OpEx and annualized CapEx, also (b) the FAC. The impact of plant lifetime on (c) OpEx and annualized CapEx, also (d) the FAC.

productivity, and energy consumption for each process. The results indicated the promising performance of MIL-160(Al) for biogas upgrading in the commercial scale (CH_4 purity of 99.9 % which consumed 903.29 kWh energy). Afterwards, a comprehensive techno-economic assessment was performed relying on industrial outcomes of VPSA processes. Interestingly, a successful development of such process for biogas upgrading is attained by the total capital expenditure (CapEx) of $14.33 million. Accordingly, the results of this study position MIL-160 (Al) as an appealing candidate for renewable energy production through the biogas upgrading.

CRediT authorship contribution statement

Mohsen Karimi: Writing – review & editing, Writing – original draft, Visualization, Validation, Software, Resources, Methodology, Investigation, Formal analysis, Data curation, Conceptualization. **Rafael M. Siqueira:** Writing – review & editing, Visualization, Validation, Software, Resources, Methodology, Investigation, Formal analysis, Data curation, Conceptualization. **Mohammad Shirzad:** Writing – review & editing, Writing – original draft, Visualization, Validation, Software, Resources, Methodology, Investigation, Formal analysis, Data curation, Conceptualization. **Alexandre F.P. Ferreira:** Validation, Resources, Methodology, Investigation. **Alírio E. Rodrigues:** Writing – review & editing, Validation, Supervision, Methodology, Investigation, Funding acquisition, Data curation, Conceptualization. **José A.C. Silva:** Writing – review & editing, Validation, Supervision, Resources, Project administration, Investigation, Funding acquisition, Data curation, Conceptualization.

Declaration of competing interest

The authors declare that they have no known competing financial interests or personal relationships that could have appeared to influence the work reported in this paper.

Acknowledgement

This work was supported by national funds through FCT/MCTES (PIDDAC): CIMO UID/00690/2025 (10.54499/UID/00690/2025) and UID/PRR/00690/2025 (10.54499/UID/PRR/00690/2025); SusTEC, LA/P/0007/2020 (DOI: 10.54499/LA/P/0007/2020)10.54499/UID/00690/202510.54499/UID/PRR/00690/202510.54499/LA/P/0007/2020Authors also would like to acknowledge Christian Serre and Farid Nouar from Institut des Matériaux Poreux de Paris, ESPCI Paris, Ecole Normale Supérieure, PSL University, Paris, France, for providing the MOF MIL-160(Al) samples.

Appendix A. Supplementary data

Supplementary data to this article can be found online at https://doi.

org/10.1016/j.seppur.2025.136571.

Data availability

Data will be made available on request.

References

[1] IPCC, Climate Change 2022: Impacts, Adaptation and Vulnerability. Contribution of Working Group II to the Sixth Assessment Report of the Intergovernmental Panel on Climate Change, Cambridge University Press, Cambridge, UK and New York, NY, USA, 2022, p. 3056.

[2] A. Naquash, M.A. Qyyum, J. Haider, A. Bokhari, H. Lim, M. Lee, State-of-the-art assessment of cryogenic technologies for biogas upgrading: energy, economic, and environmental perspectives, Renew. Sustain. Energy Rev. 154 (2022) 111826.

[3] S.F. Ahmed, M. Mofijur, K. Tarannum, A.T. Chowdhury, N. Rafa, S. Nuzhat, P.S. Kumar, D.V.N. Vo, E. Lichtfouse, T.M.I. Mahlia, Biogas upgrading, economy and utilization: a review, Environ. Chem. Lett., 2021 19:6 19 (2021) 4137–4164.

[4] R. Sangubotla, G. Gedda, J. Kim, M.G. Pang, Emerging materials and pretreatment strategies in anaerobic digestion for biogas production: a review on recent advances, limitations, and future perspectives, Ind. Crop. Prod. 236 (2025) 121939.

[5] I. Adnane, H. Taoumi, K. Lahrech, S.E. dîn Fertahi, M. Ghodbane, From waste to resource: biogas and digestate valorization strategies for sustainable energy and agriculture, Biomass Bioenergy 200 (2025) 108006.

[6] R.L. da Silva Pinto, A.C. Vieira, A. Scarpetta, F.S. Marques, R.M.M. Jorge, A. Bail, L. M.M. Jorge, M.L. Corazza, L.P. Ramos, An overview on the production of synthetic fuels from biogas, Bioresour. Technol. Rep. 18 (2022) 101104.

[7] N. Scarlat, J.F. Dallemand, F. Fahl, Biogas: developments and perspectives in Europe, Renew. Energy 129 (2018) 457–472.

[8] B. Aghel, S. Behaein, S. Wongwises, M.S. Shadloo, A review of recent progress in biogas upgrading: with emphasis on carbon capture, Biomass Bioenergy 160 (2022) 106422.

[9] A.A. Abd, M.R. Othman, S.Z. Naji, A.S. Hashim, Methane enrichment in biogas mixture using pressure swing adsorption: process fundamental and design parameters, Mater. Today Sustain. 11–12 (2021) 100063.

[10] G. Shah, E. Ahmad, K.K. Pant, V.K. Vijay, Comprehending the contemporary state of art in biogas enrichment and CO2 capture technologies via swing adsorption, Int. J. Hydrogen Energy 46 (2021) 6588–6612.

[11] T.T.T. Nguyen, G.K.H. Shimizu, A. Rajendran, CO2/N2 separation by vacuum swing adsorption using a metal–organic framework, CALF-20: multi-objective optimization and experimental validation, Chem. Eng. J. 452 (2023) 139550.

[12] M.H.V. Bahrun, A. Bono, N. Othman, M.A.A. Zaini, Carbon dioxide removal from biogas through pressure swing adsorption – a review, Chem. Eng. Res. Des. 183 (2022) 285–306.

[13] S. Keskin, T.M. van Heest, D.S. Sholl, Can metal–organic framework materials play a useful role in large-scale carbon dioxide separations? ChemSusChem 3 (2010) 879–891.

[14] M. Ding, R.W. Flaig, H.L. Jiang, O.M. Yaghi, Carbon capture and conversion using metal–organic frameworks and MOF-based materials, Chem. Soc. Rev. 48 (2019) 2783–2828.

[15] A. Permyakova, O. Skrylnyk, E. Courbon, M. Affram, S. Wang, U.H. Lee, A. H. Valekar, F. Nouar, G. Mouchaham, T. Devic, G. De Weireld, J.S. Chang, N. Steunou, M. Frère, C. Serre, Synthesis optimization, shaping, and heat reallocation evaluation of the hydrophilic metal–organic framework MIL-160(Al), ChemSusChem 10 (2017) 1419–1426.

[16] M. Karimi, A. Ferreira, A.E. Rodrigues, F. Nouar, C. Serre, J.A.C. Silva, MIL-160(Al) as a candidate for biogas upgrading and CO2 capture by adsorption processes, Ind. Eng. Chem. Res. 62 (2023) 5216–5229.

[17] R. Smith, Chemical Process Design and Integration, 2nd ed., Wiley, New Jersey, 2016. https://www.wiley.com/en-us/Chemical+Process+Design+and+Integration%2C+2nd+Edition-p-9781119990147 (accessed June 30, 2023).

[18] D.D. Do, Adsorption Analysis: Equilibria and Kinetics (with CD Containing Computer Matlab Programs), 1st ed, Imperial College Press, London, 1998, https://doi.org/10.1142/P111.

[19] S.S. Hosseini, J.F.M. Denayer, Biogas upgrading by adsorption processes: mathematical modeling, simulation and optimization approach – a review, J. Environ. Chem. Eng. 10 (2022) 107483.

[20] D.M. Ruthven, Principles of Adsorption and Adsorption Processes, 1st ed., Wiley, New York, 1984.

[21] R. Rota, P.C. Wankat, Intensification of pressure swing adsorption processes, AICHE J. 36 (1990) 1299–1312.

[22] M. Karimi, R.M. Siqueira, A.E. Rodrigues, F. Nouar, J.A.C. Silva, C. Serre, A.F. P. Ferreira, Separation of CO2/N2 onto shaped MOF MIL-160(Al) using the pressure swing adsorption process for post-combustion application, Ind. Eng. Chem. Res. 63 (2024) 8785.

[23] M. Karimi, M. Shirzad, Sustainable industrial process design for derived CO2 adsorbent from municipal solid wastes: scale-up, techno-economic and parametric assessment, Sustain. Mater. Technol. 41 (2024) e01091.

[24] CEPCI, The Chemical Engineering Plant Cost Index ® - Chemical Engineering. https://www.chemengonline.com/pci-home (accessed May 9, 2024).

[25] H.P. Loh, J. Lyons, C.W. White, Process Equipment Cost Estimation, Final Report, Pittsburgh, PA, and Morgantown, WV (United States), 2002. Doi: https://doi.org/10.2172/797810.

[26] Elmar, A.P. Heinzle, C.L. Biwer, Cooney, Development of Sustainable Bioprocesses: Modeling and Assessment, Wiley, New York, 2007.

[27] KLM Technology Group. http://www.klmtechgroup.com/.

[28] S.K. Gebremariam, Y. Al Wahedi, A. AlHajaj, L.F. Dumée, G.N. Karanikolos, System-level comparison and techno-economic evaluation of structured metal–organic framework adsorbents for post-combustion CO2 capture by vacuum/pressure swing adsorption, Chem. Eng. J. 505 (2025) 159384.

[29] M.I. Severino, E. Gkaniatsou, F. Nouar, M.L. Pinto, C. Serre, MOFs industrialization: a complete assessment of production costs, Faraday Discuss. 231 (2021) 326–341.

[30] M.I. Severino, C. Freitas, V. Pimenta, F. Nouar, M.L. Pinto, C. Serre, Cost estimation of the production of MIL-100(Fe) at industrial scale from two upscaled sustainable synthesis routes, Ind. Eng. Chem. Res. 64 (2025) 2708–2718.

[31] A. Ali Abd, M. Roslee Othman, Z. Helwani, J. Kim, An overview of biogas upgrading via pressure swing adsorption: navigating through bibliometric insights towards a conceptual framework and future research pathways, Energ. Conver. Manage. 306 (2024) 118268.

[32] L. Paz, S. Gentil, V. Fierro, A. Celzard, Assessing the performance of adsorbents for CO2/CH4 separation in pressure swing adsorption units: a review, J. Environ. Chem. Eng. 12 (2024) 114870.

[33] J. Haider, M. Abdul Qyyum, A. Riaz, A. Naquash, B. Kazmi, M. Yasin, A.S. Nizami, M. Byun, M. Lee, H. Lim, State-of-the-art process simulations and techno-economic assessments of ionic liquid-based biogas upgrading techniques: challenges and prospects, Fuel 314 (2022) 123064.

[34] A. Jabraeelzadeh, A. Gharehghani, J. Ahbabi Saray, A. Mahmoudzadeh Andwari, T.N. Borhani, Techno-economic analysis of biogas upgrading through amine scrubbing: a comparative study of different single amines, Fuel 381 (2025) 133662.

[35] F. Ferella, F. Cucchiella, I. D'Adamo, K. Gallucci, A techno-economic assessment of biogas upgrading in a developed market, J. Clean. Prod. 210 (2019) 945–957.

[36] M. Minardi, P. Marocco, M. Gandiglio, Carbon recovery from biogas through upgrading and methanation: a techno-economic and environmental assessment, J. CO_2 Util. 78 (2023).

[37] L. Lombardi, G. Francini, Techno-economic and environmental assessment of the main biogas upgrading technologies, renew, Energy 156 (2020) 440–458.

[38] S.J. Kim, Y. Song, M. Binns, J.G. Yeo, J.K. Kim, Process-integrated optimization and techno-economic analysis of membrane system for biogas upgrading: effect of membrane performance from an economic perspective, J. Membr. Sci. 713 (2025) 123286.